J. Electrochem. Sci. Eng. **10(4)** (2020) 305-315; http://dx.doi.org/10.5599/jese.774

Open Access: ISSN 1847-9286
https://pub.iapchem.org/ojs/index.php/JESE

Original scientific paper

Polymethionine modified carbon nanotube sensor for sensitive and selective determination of L-tryptophan

Nambudumada S. Prinith and Jamballi G. Manjunatha✉

Department of Chemistry, FMKMC College, Madikeri, Mangalore University Constituent College, Karnataka, India

Corresponding author: ✉manju1853@gmail.com;Tel.: +91-08272228334

Received: April 1, 2020; Revised: May 11, 2020; Accepted: May 11, 2020

Abstract

The electrochemically initiated catalytic oxidation of amino acid L-tryptophan (L-TPN) in phosphate buffer solution has been scrutinized using highly conductive polymethionine modified carbon nanotube paste sensor (PMETCNTPS) through cyclic voltammetry (CV) technique. Compared to the bare carbon nanotube paste sensor (BCNTPS), PMETCNTPS exhibited a quantifiable current signal by CV method. PMETCNTPS was found sensitive to L-TPN concentrations within the linear segment of detection range 1.5 - 8.0×10^{-5} M. By employing the calibration plot, the detection limit was determined as 6.99×10^{-7} M. In addition, PMETCNTPS was successfully exploited and validated in determining L-TPN in the pharmaceutical supplement.

Keywords

Electrochemical sensor; tryptophan; electropolymerization; cyclic voltammetry.

Introduction

Amino acids play a substantial role in biotic life and are necessary for human beings as a source of energy and for building up the proteins. Tryptophan (L-TPN) is an essential proteinogenic amino acid responsible for serving as a precursor for the neurotransmitter drug serotonin, melatonin hormone and nicotinic acid [1,2]. Therefore, the intake of L-TPN is important for humans because it has low storage in tissues and total concentration of L-TPN in the body is the least compared to all other amino acids. The small quantity of L-TPN which is necessary for human nutrition can be supplied from foods such as bananas, oats, tuna fish, milk, chocolates, dried prunes, chicken, peanuts, bread, cheese, turkey, supplements, and pharmaceutical formulations [3]. L-TPN has a major impact on the brain, since if not properly metabolized, a waste toxic product would be formed, leading to delusions and hallucinations [4]. It has already been pointed out that depletion of L-TPN levels is accompanied by weight gain, affecting the growth of kids, anxiety, chronic

insomnia, depression and pellagra [5–8]. At the other side, high intake of L-TPN leads to eosinophilia-myalgia syndrome [6]. Therefore, the availability of rapid, facile, and sensitive methods to efficiently determine the biomarker is necessary and of great significance in diagnostic aids.

A number of methods was already established to determine L-TPN, such as spectroscopy detection [9], fluorometric technique [10], high-performance liquid chromatography [11], capillary electrophoresis [12], chemiluminescence [13] and electroanalytical techniques [14–16]. The first five techniques provide accurate results but contain limitations due to poor sensitivity, non-specificity, expensive equipment, grosseness, overlong time process, and waste of high amounts of solvents for the cleaning process. All these drawbacks impede applicability of these methods significantly. Electroanalytical methods, however, are considered more appropriate for the determination of L-TPN, due to their low-priced equipment, high sensitivity, instantaneous response and easy and comfortable handling.

Among convenient electrode materials, carbon nanotubes (CNTs) have already demonstrated a significant role in biomedical, biosensing and electrochemical sensing areas. CNTs have peculiar tubular nanostructure, extraordinary chemical and electronic features, high conductivity, wide specific surface area, and possibility to alter sidewalls and ends by attaching functional groups. All these features contribute to high sensitivity and good compatibility of CNTs used as sensor electrodes. The sidewalls and ends of CNTs modified with conducting polymers have a pivotal role in recent years. The synergetic effect of two materials can enhance sensitivity, selectivity, transducing feature, biocompatibility and anti-fouling property [17–19].

In the current work, we have exploited the best features of both materials by fabricating the polymer film on a carbon nanotube sensor surface for improving the catalytic effect for the determination of L-TPN. Electro-polymerization of the monomer L-methionine (L-Met), an amino acid holding sulphur atoms in its structure, is utilized for the preparation of polymethionine carbon nanotube paste sensor (PMETCNTPS). The proposed sensor is applied for the electrochemical characterization of L-TPN and for its selective sensing in the presence of dopamine (DA). The applicability of PMETCNTPS is also validated in determining L-TPN in a pharmaceutical capsule.

Experimental

Instrumentation

Cyclic voltammetry studies were carried out with the CH-Instrument model CHI-6038E (USA), associated with a standard three-electrode system and desktop for data storage. The unmodified and polymer-modified sensors were placed as the working electrode(s), while the saturated calomel electrode (SCE), and Pt wire served as reference and auxiliary electrode, respectively. In the present work, the current measurements were considered along with the background current. All the experimental activities were performed at room temperature.

Chemicals and chemical reagents

L-tryptophan (L-TPN), L-methionine (L-Met) and orthophosphoric acid were procured from Molychem, Mumbai, India. Dopamine hydrochloride (DA) was bought from Sigma Aldrich, and silicon oil from Nice Company, Cochin, Kerala. Multiwalled carbon nanotubes (CNTs) (length of 10-30 µm and OD 30-50 nm) were purchased from Sisco Research Laboratory Pvt. Ltd., Maharashtra, India. All chemicals were of analytical grade and utilized without any purification. 25×10^{-4} M L-TPN, 25×10^{-4} M DA, and 25×10^{-3} M methionine stock solutions were prepared in deionized water. 0.1 M phosphate buffer solutions (PBS) of different pH values were prepared by mixing adequate volumes

of 0.1 M disodium phosphate and 0.1 M monosodium phosphate and adjusted to acidic pH by 0.1 M orthophosphoric solution.

Development of BCNTPS

BCNTP sensor was prepared by employing CNT powder and silicon oil with the proportion of 60:40 (w/w) and blended in an agate mortar to achieve a perfect homogenized paste. A portion of this homogenized paste was filled into the cavity (3 mm in diameter) at the tip of Teflon tube, and smoothed out the surface by rubbing it on the tissue paper.

Results and discussion

Electro-deposition of polymethionine on BCNTPS surface

Application of amino acid for electro-polymerization has a significant role in the modification of electrode surface [20]. Methionine is α-amino acid containing sulphur atom which extends the electrode feature for sensing of electroactive species [21–25]. The electropolymerization of polymethionine on BCNTPS surface can be achieved easily by CV technique. The electrochemical deposition of polymethionine was developed in 0.1 M PBS of pH 7.0, containing 1 mM methionine. Continuous potential was sweeped by 15 cycles within the potential domain -1.2 V to 1.6 V at the scan rate of 0.1 V s^{-1} (Figure 1). After finishing of electro-polymerization, the fabricated sensor was washed gently with double distilled water to take off the remnants of unreacted methionine. Thus prepared sensor electrode is depicted as PMETCNTPS.

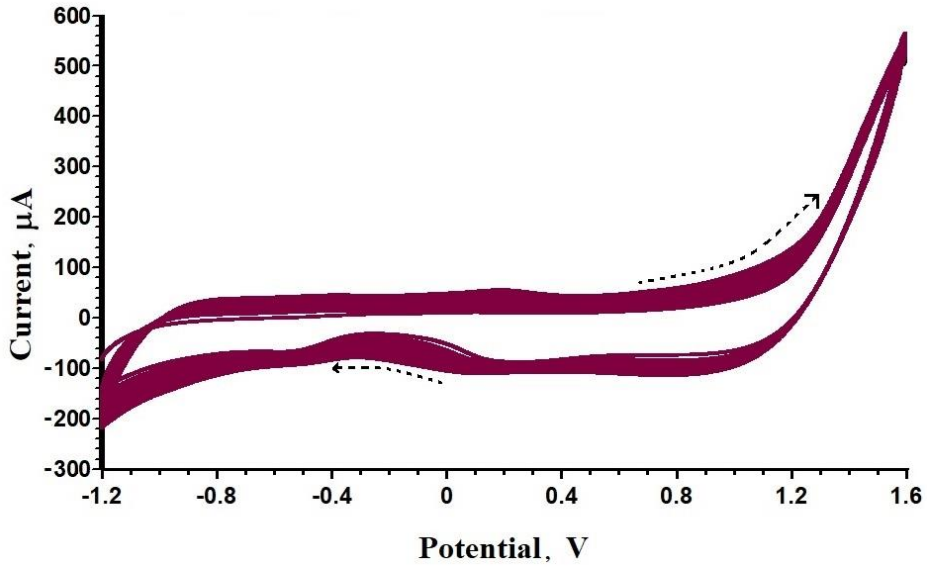

Figure 1. *Cyclic voltammograms of electro-polymerization of 1 mM L-Met in 0.1 M PBS of pH 7.0 at BCNTPS for 15 cycles at the sweep rate of 0.1 V s^{-1}.*

FE-SEM analysis of BCNTPS and PMETCNTPS

Understanding the morphology of sensing electrodes is vital as it has an impact on the kinetics of the sensor reaction, electroactive surface area, *etc*. Surface morphology was scanned using FE-SEM and presented in Figure 2. As depicted in Figure 2a, the surface of BCNTPS appears to have bundles of irregular tubular layouts. For PMETCNTPS, however, the surface morphology was changed significantly due to the physisorption of polymethionine on carbon nanotube paste sensor surface. It is noticeable from FE-SEM image in Figure 2b that PMETCNTPS surface is uniformly coated with polymethionine with the external average diameter of the nanotubes in the range of 51-56 nm. This

suggests that surface roughness was increased drastically after coating with polymethionine that is uniformly covering the surface of BCNTPS and leading to electrostatic interaction between PMETCNTPS and L-TPN molecules. The surface formed is highly porous possessing wide surface area and enhancing the conductivity of PMETCNTPS.

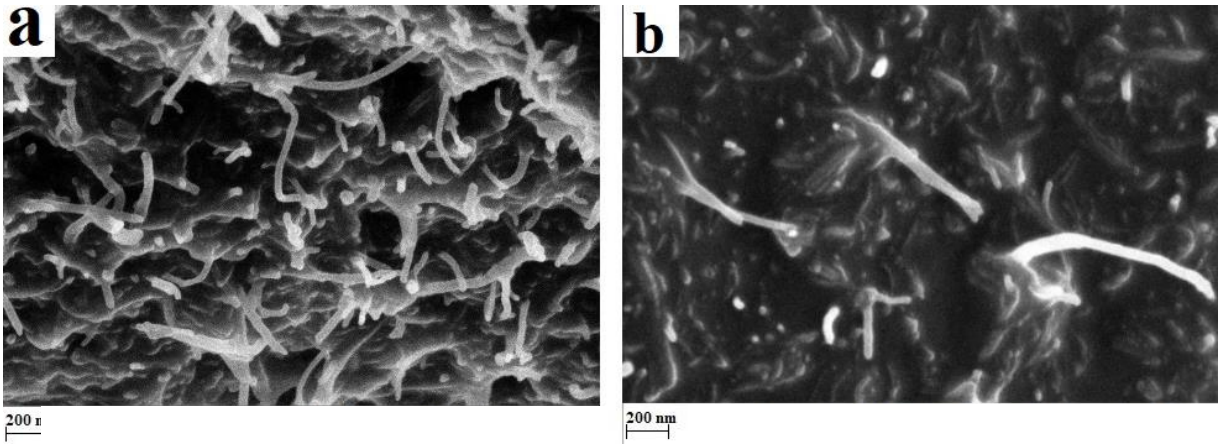

Figure 2. *FE-SEM images for (a) BCNTPS and (b) PMETCNTPS*

Assessment of surface area for BCNTPS and PMETCNTPS

It is necessary to evaluate the active surface area of the electrode that is the referent electrode parameter responsible for the reaction rate. For this purpose, CV method was applied using the charged anionic ferrocyanide, available as the potassium salt $K_4Fe(CN)_6$, and its redox reaction as a probe. Generally, thin film of polymer has the ability to attract and bind the multiple charged complex molecules. It is observed in Figure 3 that compared to BCNTPS, PMETCNTPS produced more prominent and quantifiable oxidation and reduction peaks of $[Fe(CN)_6]^{3-/4-}$ redox couple.The electrochemical active surface area was evaluated by employing Randles – Sevcik equation [26]:

$$I_p = 2.65\times10^5\, n^{3/2}\, A\, D^{½}\, v^{½}\, C \qquad (1)$$

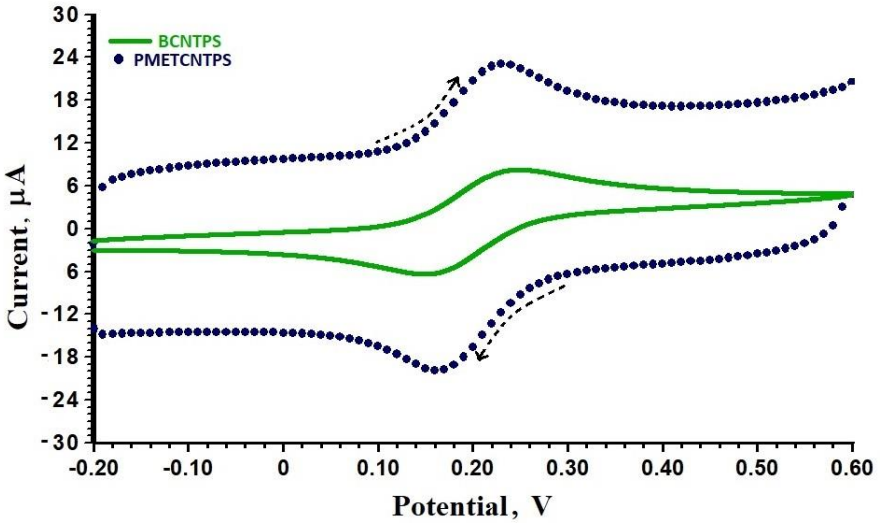

Figure 3. *Cyclic voltammograms* (0.1 V s^{-1}) o*f 1.0 mM $K_4Fe(CN)_6$ in 0.1 M KCl at BCNTPS and PMETCNTPS.*

Electrochemical activity of PMETCNTPS for determination of L-TPN

In order to compare electrochemical properties of PMETCNTPS and BCNTPS for determining 0.1 mM L-TPN in 0.1 M PBS of pH 4.0, CV technique was employed, and the results are displayed in Figure 4. A poor broad oxidation peak at 0.952 V bearing low current is spotted for L-TPN at BCNTPS

which can be associated with slow electron transfer. At PMETCNTPS, however, the response for L-TPN is enhanced with peak potential shifted negatively to 0.916 V and with 6-fold increase of the current response. This proves that the polymer fabricated electrode, possessing a great surface area, exhibits the effective electrocatalytic phenomenon to the oxidation of L-TPN. It is worth noting that in the reverse sweep the reduction peak is absent, signifying the electrochemical behavior of L-TPN as completely irreversible.

Further, to detect electrochemical sensitivity of PMETCNTPS to L-TPN, CVs were recorded in the presence and absence of L-TPN, and the results are depicted in Figure 4. Obviously, PMETCNTPS is very specific in detecting L-TPN, showing prominent anodic peak of high current. Note that in absence of L-TPN, there is no anodic peak observed at all.

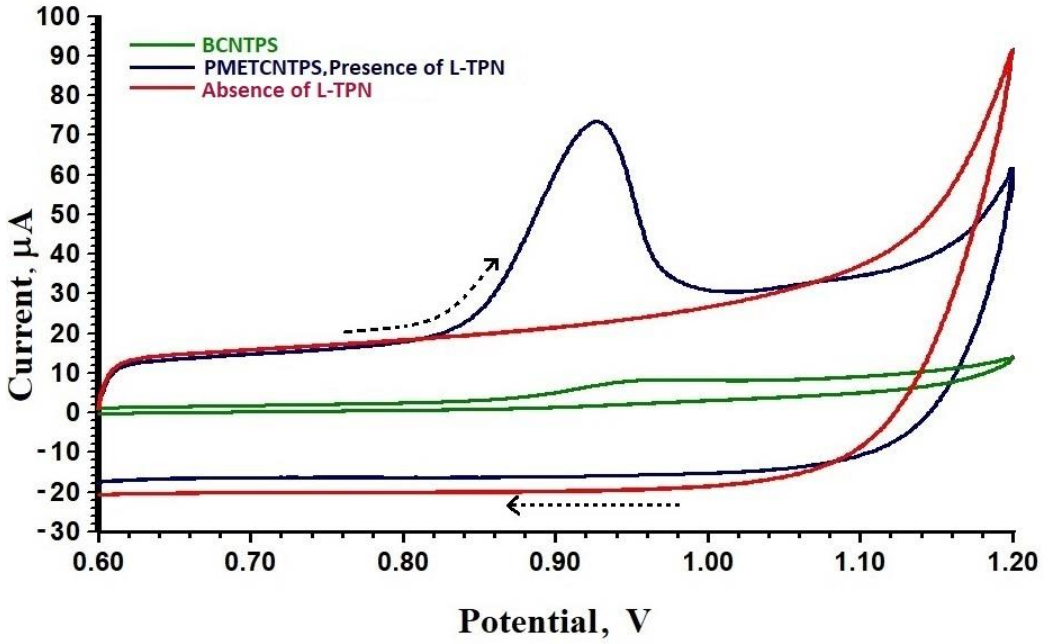

Figure 4. *CVs (0.1 V s^{-1}) in presence of 0.1 mM L-TPN in 0.1 M PBS of pH 4 at BCNTPS and PMETCNTPS, and for absence of L-TPN at PMETCNTPS.*

Optimization of experimental parameters

Impact of pH of the supporting electrolyte

Generally, the ability of the electrode surface to protonate or deprotonate depends on the variation of pH value, what could affect the capability of an electrode in regulating the electrochemical reaction. Therefore, the optimization of pH was examined by CV experiments at PMETCNTPS in 0.1 M PBS for different pH ranging from 3.0 to 7.0. The results presented in Figure 5a and particularly Figure 5b illustrate clearly that the maximum current is attained at pH 4.0 and declined gradually with further pH increase. Thus, pH 4.0 of 0.1 M PBS was chosen and set for subsequent voltammetry experiments.

As perceptible in Figure 5a, the anodic peak is shifted towards negative potential by changing pH from 3.0 to 7.0, conveying the involvement of protons in the oxidation of L-TPN. The equation estimated from the plot of anodic peak potential (E_{pa}) versus pH shown in Figure 5c is:

$$E_{pa} = 1.1026 - 0.0454\ \text{pH}\ (r = 0.976) \quad (2)$$

The slope estimated from eq. (2) is near to Nernst value of 58.5 mV/pH, demonstrating that the electrochemical reaction of L-TPN carries two electrons and two protons process.

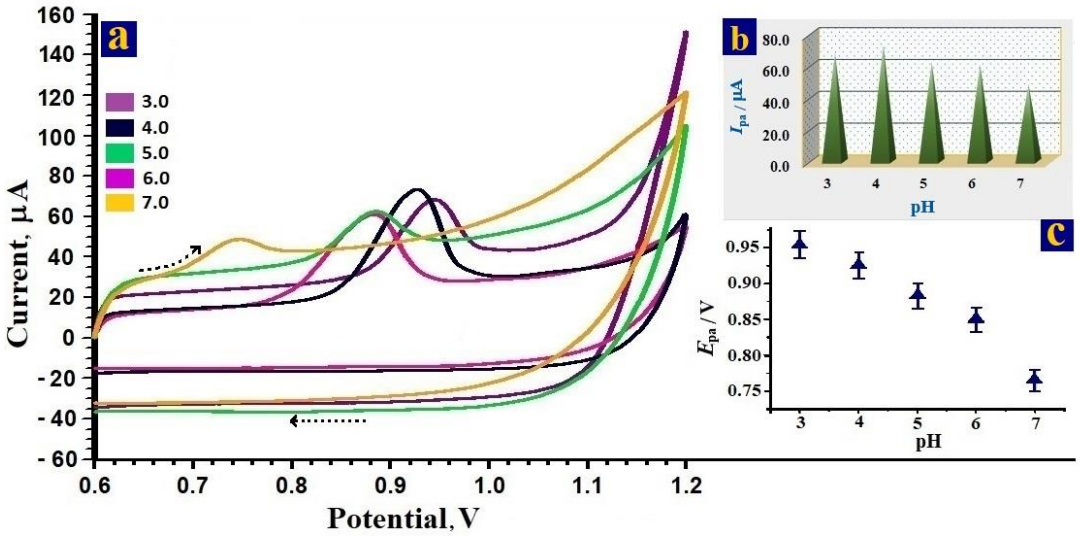

Figure 5. *(a) CVs (0.1 Vs^{-1}) of 10^{-4} L-TPN in 0.1 M PBS of different pH 3.0 -7.0 at the surface of PMETCNTPS; (b) triangular pyramid bar chart depicting* I_{pa} *for different pH; (c) graphical representation between* E_{pa} *and pH*

Impact of sweep rate

The mechanism of electrochemical reaction involved could be attained from the affiliation of peak current and sweeping rate. The impact of different sweep rates was studied for L-TPN, employing CV experiments. It can be noticed in Figure 6a that the current peak increased with increasing sweep rate.

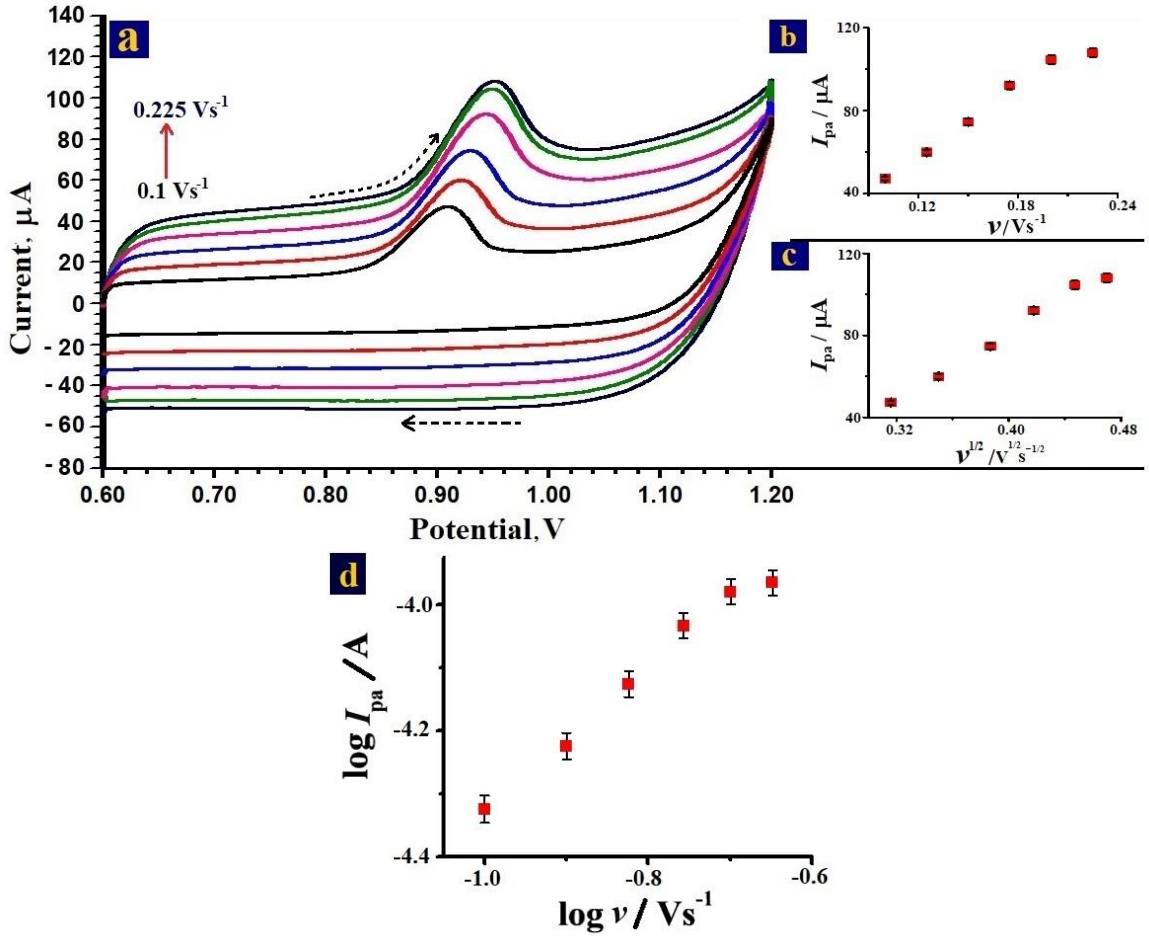

Figure 6. *(a) CVs at PMETCNTPS for 0.1 mM L-TPN in 0.1 M PBS of pH 4.0 at different potential scan rates (0.1, 0.125, 0.15, 0.175, 0.2, 0.225 V s^{-1}); (b) Plot of* I_{pa} *vs. scan rate; (c) Plot of* I_{pa} *vs. square root of scan rate; (d) Plot of log* I_{pa} *vs. log* ν

The linear dependence between peak current and sweep rate for L-TPN shown in Figure 6b was evaluated as I_{pa}= -3.48 + 520.4 ν [r = 0.988]. Similar is valid for the peak current dependence on the square root of sweep rate for L-TPN presented in Figure 6c, and evaluated to be I_{pa} = -85.54 + 418.64 $\nu^{1/2}$ [r = 0.994]. To differentiate between possible adsorption or diffusion controlled process, the plot of log (I_{pa}) and log ν was evaluated in Figure 6d and the corresponding equation is calculated to be:

$$\log I_{pa} = -3.23269 + 1.08 \log \nu \quad (r = 0.992) \qquad (3)$$

The slope of the equation (3) is 1.08 which is almost equal to the theoretical value of 1, being characteristic for the adsorption-controlled process [27–29]. This confirms that the oxidation of L-TPN is adsorption-controlled process.

The number of electrons involved in irreversible oxidation of L-TPN was calculated using Laviron expression [30,31]:

$$E_p = E^0 + (RT/\alpha nF) \ln (\alpha nF/RTK_s) + (RT/\alpha nF) \ln \nu \qquad (4)$$

Herein, E_p, E^0, *R, T, F, α, n*, and K_s are peak potential, formal potential, gas constant, temperature, Faraday constant, electron transfer coefficient, number of electrons involved, and heterogenous rate constant. The linear equation estimated from the plot of anodic peak potential (E_{pa}) versus ln ν (not shown in the figure) is defined as:

$$E_{pa} = 1.0347 + 0.05525 \ln \nu \quad (r = 0.992) \qquad (5)$$

Using the slope value of 0.05525 and α assumed to be 0.5, the number of electrons was calculated to be 2.14. This implies that the electrocatalytic oxidation of L-TPN at PMETCNTPS exhibits a two-electron transfer phenomenon. E^0 was estimated as the intercept by plotting the graph E_{pa} *vs.* ν for ν = 0. K_s estimated from the intercept of eq. (5) is 2.18 s^{-1}. The surface concentration (Γ) of PMETCNTPS was evaluated to be 3.764×10^{-9} mol/cm^2 using the following equation [32]:

$$\Gamma = Q / nFA \qquad (6)$$

In eq. (6), *Q* is charge evaluated by integration of peak area in CV data as 1.778×10^{-5} A h, *n* is number of electrons, *F* is Faraday constant (96 485.33 C mol^{-1}) and *A* is surface area of PMETCNTPS (0.03 cm^2).

Impact of number of electro-polymerization cycles of polymethionine on PMETCNTPS

In order to figure out the impact of the number of potential cycles applied during electro-polymerization of polymethionine on the anodic peak current of L-TPN, current responses at PMETCNTPS formed by different numbers of cycles of electro-polymerization were recorded. CVs presented in Figure 7a show that as the number of polymerization cycles increased from 5 to 15.

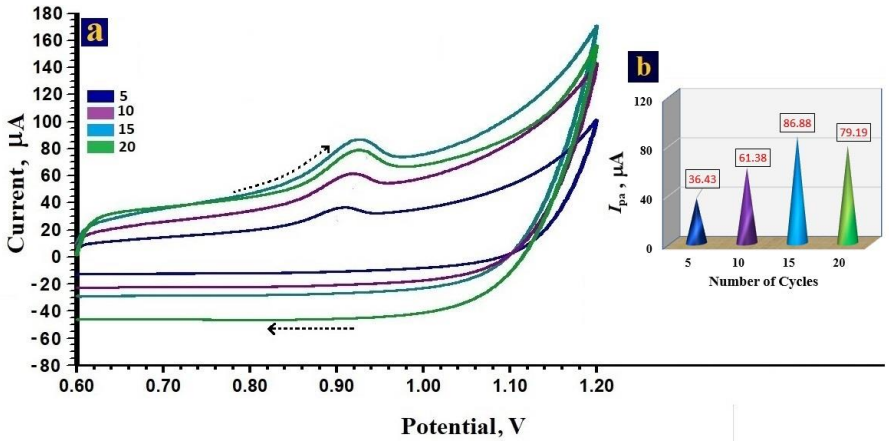

Figure 7. *(a) CVs (0.1 V s^{-1}) for 0.1 mM L-TPN in 0.1 M PBS of pH 4.0 at PMETCNTPS formed by different number of electro-polymerization cycles on CNTPS; (b)Typical conical chart representation of* I_{pa} vs. *number of polymerization cycles*

The current peak was firstly enhanced dramatically, while for more than 15 cycles, the current peak was declined (Figure 7b). This might be related to the increase of the polymer film thickness, resulting in the hindrance of charge transfer at the surface of the electrode.

Concentration variation of L-TPN at PMETCNTPS

For the quantitative determination of L-TPN at PMETCNTPS, cyclic voltammetry was also employed. The voltammograms unveiled the linear dependence between peak current increase and increase of L-TPN concentration. As observed in Figure 8, two linear segments were obtained in the range of 2 – 10 μM and 15 - 80 μM, respectively. Here, the second linearity was chosen for the further analysis as it has the wide linear segment range described by the following regression equation:

$$I_{pa} = 36.37258 + 0.60017\ C_{TPN}\ (r = 0.997) \quad (7)$$

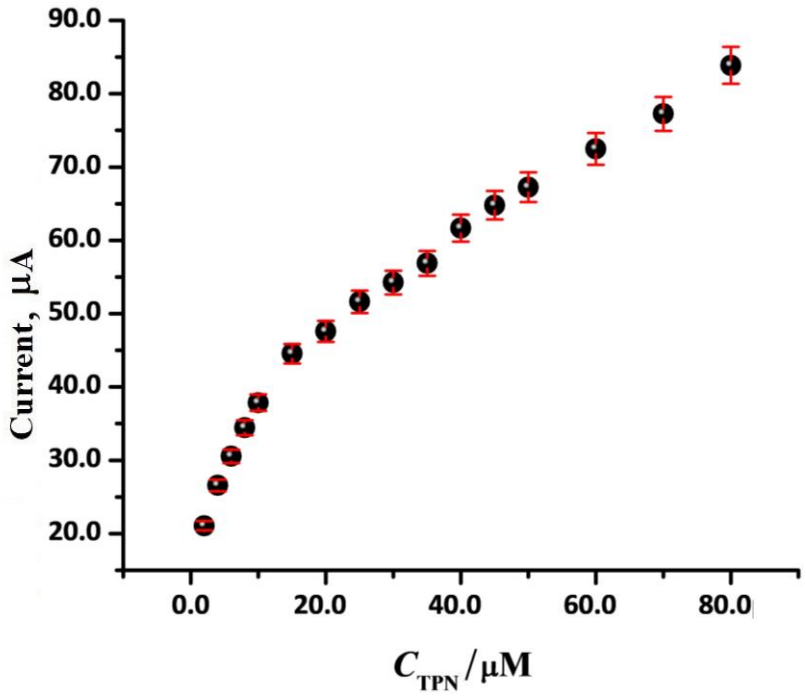

Figure 8. *Calibration plot at PMETCNTPS showing anodic peak current vs. concentration of L-TPN*

Detection limit (LOD) and quantification limit (LOQ) were estimated to be 0.699 μM and 2.33 μM. LOD and LOQ values were estimated applying the following equations[19,29]:

$$LOD = 3S_d / M;\ \ LOQ = 10\ S_d / M \quad (8)$$

In eq. (8), S_d is standard deviation evaluated from the blank and M is the slope of the calibration plot. LOD values and linear ranges of concentration of L-TPN already obtained for various electrodes are compared in Table 1, suggesting high efficiency of the present PMETCNTP sensor.

Table 1. *Comparison of efficacy of PMETCNTPS with other reported sensors for determination of L-TPN*

	Modified Sensor	Methods	Linear Range, μM	Detection Limit, μM	Ref.
1	CPE	CV DPV	29.1 – 82.6 2.06 - 30	4.66 1.66	[33]
2	BDD	DPV	20 -1000	10	[34]
3	GNP/CILE	SWV	5 - 900	4	[35]
4	CILE	CV	8-1000	4.8	[36]
5	PMETCNTPS	CV	15 - 80	0.69	This work

CPE: carbon paste electrode; BDD: boron-doped diamond electrode; GNP/CILE: gold nanoparticle – modified carbon ionic liquid electrode; DPV: differential pulse voltammetry; SWV: square wave voltammetry.

Repeatability, reproducibility, and stability of PMETCNTPS

The stability was inspected for repetitive 25 cycles for 0.1 mM L-TPN in 0.1 M PBS of pH 4.0 at the fabricated PMETCNTPS sensor. The resulting percentage of degradation is calculated by applying the following expression [33]:

$$\text{Degradation, \%} = (I_{p(n)} / I_{p(1)})\ 100 \quad (9)$$

In eq. (9), $I_{p(n)}$ is anodic peak current measured in n^{th} measurement, while the first measured anodic peak current is labeled as $I_{p(1)}$. The calculated percentage of degradation is 1.05, suggesting high stability of the fabricated sensor electrode. The reproducibility and repeatability of PMETCNTPS were estimated as 4.3 and 1.6 %, respectively.

Simultaneous determination of L-TPN in presence of another electroactive species

Dopamine (DA) is a neurotransmitter drug and one of the happy hormones. L-TPN is the precursor for another happy hormone and the neurotransmitter drug, serotonin. Therefore, DA and L-TPN coincide in the extra-cellular fluid of the central nervous system and serum. Here, the fabricated working sensor PMETCNTPS was inspected for the simultaneous determination of these two electroactive species. It is observed and portrayed in Figure 9 that by showing low and broad peak, BCNTPS clearly failed in simultaneous determining of two electroactive species. On the contrary, BCNTPS modified by polymethionine presents two well-separated and enhanced current signals for both DA and L-TPN. This proves that PMETCNTPS is highly selective sensor.

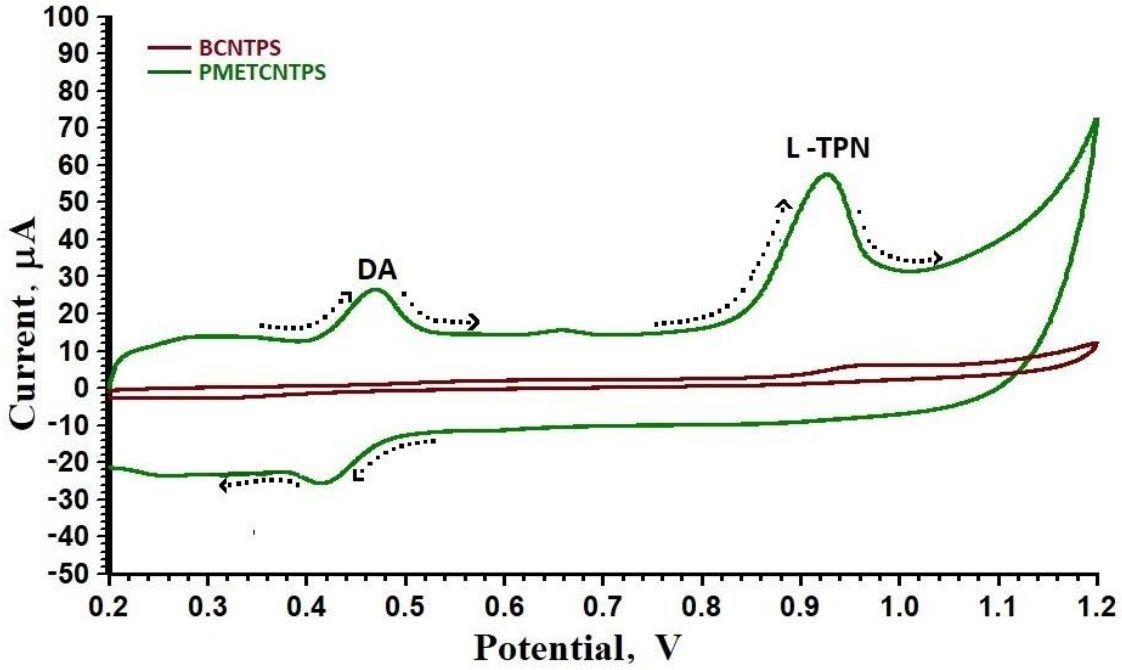

Figure 9. *CVs (0.1 V s^{-1}) for the mixture of 0.1 mM L-TPN and 0.1 mM DA in 0.1 M PBS of pH 4.0 at BCNTPS and PMETCNTPS.*

Analysis of L-TPN capsule

The practical applicability of PMETCNTPS was evaluated for the commercial medicinal capsule of L-TPN from Advance Nutratech. The amount of L-TPN in the capsule was labeled as 500 mg. The solution of specified concentration was prepared by a powdered capsule and examined by CV method. A known volume of L-TPN capsule solution was diluted with 0.1 M PBS of pH 4.0. The standard addition method was utilized for examining the pharmaceutical sample. The results are summarized in Table 2, showing also high percentage recovery within the range of 97.5 to 98.6 %.

Table 2. *Application of PMETCNTPS for detection of L-TPN in L-TPN capsule.*

Sample	Sample No.	Added L-TPN, μM	Found L-TPN, μM	Recovery, %
L -Tryptophan Capsule	1	5.2	5.096	98
	2	10.4	10.25	98.6
	3	15.6	15.21	97.5

Conclusions

A new sensor electrode is prepared by electro-polymerization of L-methionine on carbon multiwalled nanotube paste surface (PMETCNTPS) and successfully applied for the determination of L-tryptophan (L-TPN). Compared to the basic electrode, cyclic voltammetry results of the fabricated PMETCNTPS revealed increased current and negative shift of anodic peak, demonstrating good electrocatalytic activity toward electro-oxidation of L-TPN. The corresponding electrochemical reaction was found irreversible, carrying two-electron and two-proton transfer and controlled by the adsorption process. Cyclic voltammograms measured under optimal experimental conditions, showed good linear dependence between oxidation peak current and concentration of L-TPN within wide linear range of 15 μM – 80 μM and possessing the detection limit of 0.69 μM. The developed PMETCNTPS showed high sensitivity, high selectivity, and high specificity when L-TPN was measured in presence of dopamine (DA). The projected sensor electrode disclosed high percentage recovery which may be applied in drug formulations and pharmacokinetics study.

Acknowledgements: *We convey our gratitude to the VGST, Bangalore under Research Project No.KSTePS/VGST-KFIST(LI)2016-2017/GRD-559/2017-18/126/333, 21/11/2017 for their financial support.*

References

[1] M. Kooshki, H. Abdollahi, S. Bozorgzadeh, B. Haghighi, *Electrochimica Acta* **56** (2011) 8618–8624.
[2] R. N. Goyal, S. Bishnoi, H. Chasta, M. A. Aziz, M. Oyama, *Talanta* **85** (2011) 2626–2631.
[3] D. M. Richard, M. A. Dawes, C. W. Mathias, A. Acheson, N. Hill-Kapturczak, D. M. Dougherty, *International Journal of Tryptophan Research* **2** (2009) 45–60.
[4] A. Özcan, Y. Şahin, *Biosensors and Bioelectronics* **31** (2012) 26–31.
[5] M. Tessema, N. S. Gunaratna, I. D. Brouwer, K. Donato, J. L. Cohen, M. McConnell, T. Belachew, D. Belayneh, H. De Groote, *Nutrients* **10(11)** (2018) Art.ID 1776, http://doi.org/10.3390/nu10111776.
[6] C. Hudson, S. P. Hudson, T. Hecht, J. Mackenzie, *Nutritional Neuroscience* **8** (2005) 121–127.
[7] T. A. Jenkins, J. C. D. Nguyen, K. E. Polglaze, P. P. Bertrand, *Nutrients* **8(1)** (2016) Art. ID 56, http://doi.org/10.3390/nu8010056.
[8] H. Vannucchi, J. A. Mello de Oliveira, J. E. Dutra de Oliveira, *The American Journal of Clinical Nutrition* **35** (1982) 1368–1374.
[9] H. Edelhoch, *Biochemistry* **6** (1967) 1948–1954.
[10] M. Shinttzky, R. Goldman, *European Journal of Biochemistry* **3** (1967) 139–144.
[11] S. A. Çevikkalp, G. B. Löker, M. Yaman, B. Amoutzopoulos, *Food Chemistry* **193** (2016) 26–29.
[12] R. M. Latorre, J. Saurina, S. Hernández-Cassou, *Journal of Chromatographic Science* **37** (1999) 353–359.
[13] S. Li, M. Xing, H. Wang, L. Zhang, Y. Zhong, L. Chen, *RSC Advances* **5** (2015) 59286–59291.
[14] B. Fang, Y. Wei, M. Li, G. Wang, W. Zhang, *Talanta* **72** (2007) 1302–1306.
[15] P. Prabhu, R. S. Babu, S. S. Narayanan, *Colloids and Surfaces B: Biointerfaces* **87** (2011) 103–108.
[16] K. Huang, C. Xu, J. Sun, W. Xie, L. Peng, *Analytical Letters* **43** (2009) 176–185.
[17] S. Hu, C. Hu, *Journal of Sensors* (2009), Article ID 187615, doi:10.1155/2009/187615
[18] H. Beitollahi, M. Safaei, S. Tajik, *Journal of Electrochemical Science and Engineering* **9** (2019) 27–43.
[19] J. G. Manjunatha, *Journal of Electrochemical Science and Engineering* **7** (2017) 39–49.
[20] G. Tigari, J. G. Manjunatha, *Journal of Analysis and Testing* **3** (2019) 331–340.

[21] S. Cheemalapati, B. Devadas, S. M. Chen, *Journal of Colloid and Interface Science* **418** (2014) 132–139.
[22] B. K. Chethana, Y. Arthoba Naik, *Analytical Methods* **4** (2012) 3754–3759.
[23] B. N. Chandrashekar, W. Lv, G. K. Jayaprakash, K. Harrath, L. W. Y. Liu, B. E. K. Swamy, *Chemosensors* **7(2)** (2019) Art.ID 24, http://doi.org/10.3390/chemosensors/7020024.
[24] R. Ojani, A. Alinezhad, Z. Abedi, *Sensors and Actuators B: Chemical* **188** (2013) 621–630.
[25] Y. Wang, X. Ouyang, Y. Ding, B. Liu, D. Xu, L. Liao, *RSC Advances* **6** (2016) 10662–10669.
[26] N. Hareesha, J. G. Manjunatha, *Materials Research Innovations* (2019) http://doi.org/10.1080/1432-8917.2019.1684657.
[27] H. Beitollahi, Z. Dourandish, S. Tajik, M.R. Ganjali, P. Norouzi, F. Faridbod, *Journal of Rare Earths* **36** (2018) 750–757.
[28] S. D. Bukkitgar, N. P. Shetti, *ChemistrySelect* **1** (2016) 771–777.
[29] N. S. Prinith, J. G. Manjunatha, C. Raril, *Analytical and Bioanalytical Electrochemistry* **11** (2019) 742–756.
[30] X. Liu, L. Luo, Y. Ding, D. Ye, *Bioelectrochemistry* **82** (2011) 38–45.
[31] L. Fotouhi, M. Fatollahzadeh, M. M. Heravi, *International Journal of Electrochemical Science* **7** (2012) 3919–3928.
[32] P. A. Pushpanjali, J. G. Manjunatha, M. T. Shreenivas, *ChemistrySelect* **4** (2019) 13427–13433.
[33] M. M. Charithra, J. G. Manjunatha, *Journal of Electrochemical Science and Engineering* **10** (2019) 29-40.
[34] A. R. Fiorucci, É. T. G. Cavalheiro, *Journal of Pharmaceutical and Biomedical Analysis* **28** (2002) 909–915.
[35] G. Zhao, Y. Qi, Y. Tian, *Electroanalysis* **18** (2006) 830–834.
[36] A. Safavi, S. Momeni, *Electroanalysis* **22** (2010) 2848–2855.